

# Hybrid successive continuous wave interference cancellation scheme for global positioning system receivers

Ying-Ren Chien

*Adaptive and Autonomous Communication Laboratory, Department of Electrical Engineering, National Ilan University, No. 1, Sec. 1, Shen-Lung Road, I-Lan City 26041, Taiwan*  
E-mail: yrchien@niu.edu.tw; curtis.chien@gmail.com

Published in *The Journal of Engineering*; Received on 11th April 2013; Accepted on 30th May 2013

**Abstract:** The authors propose a hybrid successive continuous wave interference (CWI) cancellation scheme for GPS receivers. The proposed hybrid scheme successively detects and estimates CWIs in the time domain and nulls the estimated contaminated frequencies in the frequency domain. An adaptive second-order infinite impulse response (IIR) filter to perform the CWI detection and estimation is devised. One IIR filter is able to estimate one CWI in each iteration. Then, the detected CWI is fed back to the excision module in the frequency domain. Therefore, the hybrid scheme can successively null multiple CWIs. Moreover, the proposed architecture allows additional cascading of IIR filters to handle multiple CWIs simultaneously. Unlike the existing frequency-domain approach, CWI estimation does not rely on the statistical values in the frequency domain. Therefore the proposed hybrid scheme can be implemented using a fast Fourier transform (FFT) with fewer points. Simulation results show that the proposed hybrid scheme can operate normally with only a 256-point FFT and can perform better than the conventional  $N$ -sigma and consecutive mean excision algorithms in terms of the effective signal to interference plus noise ratio of the acquisition results.

## 1 Introduction

Among future spectrum-demanding services, terrestrial broadband signals are the most likely to jam global positioning system (GPS) receivers [1]. Although GPS receivers have an inherent anti-jamming ability due to their spreading spectrum characteristics, the performance of GPS receivers degrades severely as jamming signals exceed the system's anti-jamming ability. Of the different types of harmful jamming sources, continuous wave interference (CWI) and pulsed CWI have been shown to have the most severe impacts on the quality of the received GPS signal [2]. Moreover, such interference can easily overwhelm a GPS receiver's analogue-to-digital converter (ADC) at the analogue front end, paralyse the operation of GPS receivers [3] and degrade the performance of code tracking loops [4]. Furthermore, the number of people who use GPS-enabled mobile devices to execute location-based applications is increasing. A jamming attack may cause these mobile devices to lose GPS signals [5]. Therefore, a GPS receiver with low-computational complexity CWI detection and rejection capabilities is required.

The most often used CWI rejection techniques operate in either the frequency domain [6–12] or the time domain [13–17]. Some approaches work in both the frequency and time domains, that is, hybrid-domain approaches [18, 19].

For the frequency-domain approaches, a partial coefficient-updating algorithm is designed to adaptively update  $N$  sets of interference rejection blocks [6], statistical hypothesis testing is devised to detect GPS interference [7] and a wavelet transform-based approach is proposed to suppress CWIs [8].

Capozza *et al.* [9] proposed an  $N$ -sigma excision algorithm to null CWIs in the frequency domain. The  $N$ -sigma algorithm exploits the fact that the received GPS signals have an approximately Gaussian distribution in the absence of narrow-band jamming. In this un-jammed case, most received signal magnitudes are less than two standard deviations above the mean magnitude. Hence, the  $N$ -sigma excision algorithm adaptively determines the excision threshold and excises the frequency bins with magnitudes above the threshold from each fast Fourier transform (FFT) data block. Feng *et al.* [10] proposed a new  $N$ -sigma algorithm based on a fuzzy threshold. Similarly, a consecutive mean excision (CME) algorithm

[11, 12] exploits the fact that the magnitude spectrum of a received signal is approximately Rayleigh distributed with two degrees of freedom in the absence of narrow-band jamming. All frequency bins are iteratively divided into two classes: inlier and outlier. The frequency bins belonging to the inlier class are treated as clean signals, and those belonging to the outlier class are treated as contaminated signals. A threshold parameter, which is determined a priori based on the assumption of desired signal set statistics, is used to classify whether a frequency bin belongs to the inlier or outlier class. Both  $N$ -sigma and CME algorithms require calculation of the statistical value of the frequency-domain data to determine the threshold. To obtain a more accurate threshold, a higher frequency resolution is preferred, which means that more FFT points are required.

For time-domain approaches, Rusch and Poor [13] proposed an enhanced non-linear method to suppress the interferences. However, this approach requires a non-linear function,  $\tanh$ , which is computationally intensive. Moreover, the performance depends on the correctness of the feedback data. In [14], the authors utilised a notch filter to reduce spurs and combined a feedback filter to cancel intersymbol interferences caused by the notch filter. However, the performance may degrade because of decision errors. Ma *et al.* [15] proposed an adaptive all-pass-based notch filter to reject CWIs. However, hardware cost may increase because the information of the covariance matrix and its inverse are required during the adaptation process. Borio *et al.* [16] proposed two-pole and multi-pole notch filters to detect and mitigate CWIs. The authors adopted the location of the zeros of the notch filters to detect CWIs. In [17], the authors have proposed a CWI-detectable adaptive notch filter module, which is composed of a second-order infinite impulse response (IIR) filter, to mitigate one CWI in the time domain. However, the non-linear phase property associated with the IIR filters incurs tracking biases if the notch bandwidth parameter is improperly chosen. For hybrid-domain approaches, Villanti *et al.* [18] proposed a joint time–frequency domain architecture that estimates the instantaneous interferer frequency and passes the estimation to an adjustable FIR filter to cancel single-tone interference. Likewise, Borio *et al.* [19] proposed a time–frequency algorithm in which a time–frequency

representation is used to estimate the jamming frequency and an IIR filter is equipped to remove interferences in the time domain. However, the short-time Fourier transform must be calculated to construct the discrete time spectrogram.

To gain advantages of signal processing in both the frequency and time domains, we propose a novel hybrid approach that sequentially detects the jamming frequency in the time domain and removes the polluted frequency bins in the frequency domain. Our hybrid approach has the following advantages. First, we adopt only one simple IIR filter to detect the strongest jamming at the receiver side. By properly choosing the bandwidth of the IIR filter, we can detect the jamming frequency with a high resolution. If more jamming frequencies need to be simultaneously estimated, we can cascade more IIR filters. Second, the signals passed to the IIR filter are only used to detect the jamming frequency. Therefore, the non-linear phase of the IIR filter does not affect subsequent signal processing, such as acquisition and tracking. Third, our architecture does not need to calculate statistical values with frequency data, instead removing the frequency bins according to the jamming frequency estimation feedback by the time domain IIR filter. Compared with  $N$ -sigma and CME algorithms, our architecture performs better, in terms of acquisition results, with fewer FFT points.

The rest of this paper is organised as follows: Section 2 describes the system model. The proposed hybrid successive interference cancellation (SIC) scheme is presented in Section 3. Section 4 presents simulation results and makes comparisons with [10, 11]. Finally, we conclude this paper in Section 5.

## 2 Proposed hybrid-domain system model

Fig. 1 shows a hybrid-domain GPS anti-jamming system model. In addition to the receiver analogue front end and the digital signal processing (DSP) back end, the proposed anti-jamming system consists mainly of the frequency-domain interference suppression (FDIS) and time-domain interference detection and estimation (TDIDE) blocks. The TDIDE block is able to detect and estimate one single jamming frequency at each iteration. The estimated jamming frequency is then nulled by the FDIS block, which is able to null multiple frequency bins simultaneously. The TDIDE block then successively estimates the residual CWI contained in the output of the FDIS block. We call this procedure the hybrid successive CWI cancellation scheme. The details of the received signal model, FDIS block and TDIDE block are described as follows.

### 2.1 Received signal models

The down-converted received signal  $\tilde{r}(t)$  is composed of the filtered version of a transmitted GPS signal  $s(t)$ , the additive white Gaussian noise (AWGN)  $w(t)$  with zero mean and two-sided power spectral density  $N_0/2$ , and the CWI  $j(t)$ . The transmitted GPS signal is

assumed to be

$$s(t) = \sqrt{2P_s} D(t) C(t) \cos(2\pi f_{L1} t + \theta) \quad (1)$$

where  $P_s$  is the power of signals with coarse acquisition (C/A) code  $C(t)$  with chip rate  $R_c = 1.023$  MHz;  $D(t)$  is the navigation data;  $\theta$  is the phase delay; and  $f_{L1}$  denotes the carrier frequency of L1 (1575.42 MHz).

The jamming signals are assumed to be multi-tone CWIs and can be expressed as

$$j(t) = \sum_{i=1}^K \sqrt{2P_{J,i}} \cos(2\pi f_{J,i} t + \theta_{J,i}) \quad (2)$$

where  $K$  is the number of CWIs and  $P_{J,i}$ ,  $f_{J,i}$  and  $\theta_{J,i}$  are the power, frequency and phase delay of the  $i$ th jamming signal, respectively. The jamming-to-signal ratio (JSR) for each jamming signal is defined as

$$\text{JSR}_i = 10 \log_{10} \left\{ \frac{P_{J,i}}{P_s} \right\} \quad (3)$$

Owing to the orthogonality of the C/A code, a GPS receiver is able to process the signal transmitted by different satellites individually. Therefore, without loss of generality, the received signal  $\tilde{r}(t)$  can be simplified to consider a single satellite at a time. After down converting to the intermediate frequency (IF), the down-converted signal can be expressed as

$$\tilde{r}(t) = s'(t) + w(t) + j(t) \quad (4)$$

where

$$s'(t) = \sqrt{2P_s} D(t - \tau) C(t - \tau) \cos[2\pi(f_d + f_{IF})t + \theta]$$

where  $\tau$  is the delay introduced by the transmission channel of the satellite;  $f_d$  and  $\theta$  are the corresponding Doppler frequency and phase offset, respectively; and  $f_{IF}$  is the IF of 4.092 MHz.

After bandpass filtering and signal amplification, the signal,  $r(t)$ , at the input of the ADC can be expressed as

$$r(t) = \{[s'(t) + w(t) + j(t)] * h_{BP}(t)\} G(t) \triangleq \tilde{s}(t) + \tilde{w}(t) + \tilde{j}(t) \quad (5)$$

where  $h_{BP}(t)$  is the impulse response of the bandpass filter (BPF), and  $G(t)$  is the gain of the variable gain amplifier (VGA); '\*' denotes the convolution operation.  $r(t)$  is then sampled with the rate  $1/T_s$ , which is four times  $f_{IF}$ . The sampled values  $r[n] = r(nT_s)$

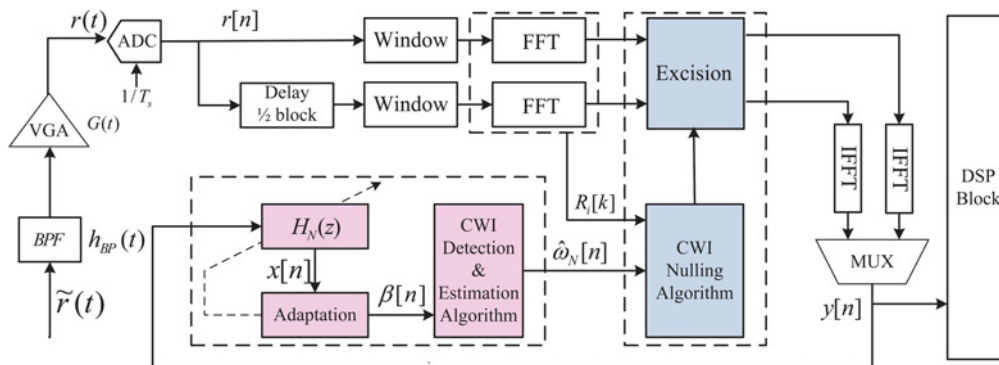


Fig. 1 Hybrid-domain GPS anti-jamming system model

are then input to the frequency-domain interference suppression (FDIS) block.

## 2.2 FDIS block

As discussed in [9], the FDIS approach may cause spectral leakage issues. Although windowing techniques can abate the spectral leakage issue, these techniques result in signal-to-noise ratio (SNR) losses. The SNR loss results from an  $N$ -point window function  $w(n)$ , defined as

$$L_w \triangleq \frac{\sum_{n=0}^{N-1} w(n)}{N \sum_{n=0}^{N-1} w^2(n)} \quad (6)$$

A trade-off between the SNR loss and the effectiveness of the spectral containment for a CWI must be made when we choose a proper window function. A good window function for a GPS application is a four-term Blackman–Harris window, which can maintain continuous wave frequency containment but with an SNR loss  $L_w = 3$  dB. Fortunately, we can compensate for the SNR loss using the well-known 50% overlapping technique [20]. With 50% overlapping compensation, the loss of the SNR  $L_w$  caused by the four-term Blackman–Harris window is reduced from 3 to 0.6 dB [9]. The overlapping compensation is provided by adding a second signal path with a  $1/2$  delay block. As shown in Fig. 1, the received sampled signals  $r[n]$  are supplied in two paths offset by  $N_F/2$  samples with respect to each other. The signals along these two paths are then separately windowed and translated into the frequency domain by  $N_F$ -point FFT blocks. These signals can be expressed as follows

$$R_1[k] = \sum_{n=0}^{N_F-1} r[n]w[n]e^{-j2\pi nk/N_F} \quad (7)$$

$$R_2[k] = \sum_{n=0}^{N_F-1} r[n - N_F/2]w[n]e^{-j2\pi nk/N_F} \quad (8)$$

where  $N_F$  denotes the number of FFT points and  $w[n]$  denotes the window function.

To suppress the jamming signals in the frequency domain, the excision unit nulls the frequency bins in a nulling pool  $J$ , which is provided by the CWI nulling algorithm. After the excision process, the  $N_F$ -point inverse FFT (IFFT) blocks translate the frequency domain signals back to the time domain. Finally, a multiplexer (MUX) combine the signals on these two paths, resulting in the combined signals expressed as follows

$$y[n] = \frac{1}{N_F} \sum_{k=0}^{N_F-1} (X_1[k] + X_2[k])e^{j2\pi nk/N_F} \quad (9)$$

The combined signals  $y[n]$  pass not only to the following DSP block, which is mainly composed of acquisition, tracking and navigation processing blocks, but also to a time-domain interference detection and estimation block.

## 2.3 TDIDE block

A TDIDE block determines the frequency bins that should be excised in the FDIS block. We propose using a simple but effective second-order adaptive IIR notch filter, with transfer function  $H_N(z)$ , as a module to detect and estimate the jamming frequency [17]. One module can detect the strongest CWI presents in its input. Our CWI detection algorithm uses the internal status during an adaptation processing with the IIR filter to detect whether a CWI is present. According to the CWI detection results, a CWI estimation algorithm then provides an estimated frequency of the detected CWI  $\hat{f}_j[n]$ . By feeding back  $\{y[n]\}$  to the TDIDS block, the proposed

hybrid-domain architecture can successively detect residual CWIs and eventually null all CWIs using the FDIS block. More details about the proposed CWI detection, estimation and nulling algorithms are described in Section 3.

## 2.4 Performance evaluation metrics

To evaluate the anti-jamming capability with various algorithms, we adopt the signal to interference plus noise ratio (SINR), the detection probability and the effective SINR as the performance evaluation metrics. These three metrics are defined as follows.

Let SINR  $\Gamma$  denotes the power ratio of the main peak value to other off-peak values after the received signals are despreaded

$$\Gamma \triangleq \frac{\eta[k]}{\text{AVG}_{n \neq k, k \pm 1} \{\eta[n]\}} \quad (10)$$

where  $k = \text{argmax}_n \{\eta[n]\}$  denotes the index of the peak of the correlation output,  $\{\eta[n]\}$  denotes the output of the circular cross-correlation between the input of the acquisition block and the C/A code, and  $\text{AVG}\{\cdot\}$  denotes the average operation. Note that a higher  $\Gamma$  results in higher quality despreaded signals. Moreover, we define the effective SINR  $\tilde{\Gamma}$  as

$$\tilde{\Gamma} \triangleq \Gamma \times P_d \quad (11)$$

where  $P_d$  is the detection probability of GPS signals.

## 3 Proposed hybrid SIC scheme

In this section, we first describe how to use an adaptive second-order IIR filter to notch the jamming signals embedded in its input. The architecture of the adaptive IIR filter and the associated adaptive algorithm are also given. Second, we mathematically derive the CWI detection and estimation algorithm. After collecting  $N_\beta$  points of  $y[n]$ , we calculate the sample variance of the state variable associated with the adaptive IIR filter. This statistical value is then used to detect the presence of CWI. If CWI is present, the statistic value can be used to estimate the jamming frequency. The detected jamming frequency is recorded in a nulling pool. Third, before excising the frequency bins in the nulling pool, a CWI nulling algorithm verifies that all of the estimated jamming bins are still available by checking the amplitude of these frequency bins. Finally, we extend the proposed architecture to a concurrent CWI detection version so that multiple CWIs can be detected at each iteration.

### 3.1 Architecture of the adaptive IIR filter

Fig. 2 shows the block diagram of the second-order adaptive IIR notch filter with the input signals  $u[n]$ , output signals  $y[n]$  and adaptive signals  $x[n]$ . The filter is stable if the absolute values of both  $\alpha$  and  $\beta$  are smaller than 1. The Z-domain transfer function of the

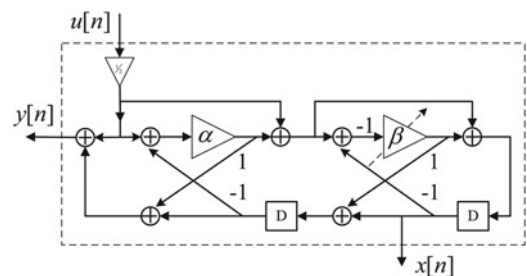


Fig. 2 Block diagram of the second-order ANF

notch filter is characterised by

$$H_N(z) \triangleq \frac{Y(z)}{U(z)} = \frac{1 + \alpha}{2} \frac{1 - 2\beta z^{-1} + z^{-2}}{1 - \beta(1 + \alpha)z^{-1} + \alpha z^{-2}} \quad (12)$$

where  $Y(z)$  and  $U(z)$  are the  $Z$ -transform representations for  $y[n]$  and  $u[n]$ , respectively. The  $-3$  dB bandwidth  $B$  and notch frequency  $\omega_N$  are controlled by  $\alpha$  and  $\beta$ , respectively, and can be expressed as [21]

$$\alpha = \frac{1 - \tan(B/2)}{1 + \tan(B/2)} \quad (13)$$

$$\beta = \cos(\omega_N) \quad \text{with} \quad \omega_N \in [0, \pi] \quad (14)$$

Note that the adaptations for the  $-3$  dB bandwidth and notch frequency are independent of each other. If the CWI appears in the passband of the GPS signal, the ANF will notch both CWI and GPS signals. We fix the parameter  $\alpha$  and only adapt  $\beta$ . The choice of  $\alpha$  depends on the desired resolution of the multiple CWI detection and on the frequency resolution of the FDIS block. As the absolute value of  $\alpha$  moves closer to 1, the  $-3$  dB bandwidth decreases; that is, the resolution to distinguish multiple CWIs increases.

The intuition behind the adaptation algorithm is explained as follows. If the CWI has been notched,  $y[n] + w[n]$  and  $x[n]$  must hold. In this case, the cross-correlation between  $j[n]$  and  $s[n] + w[n]$  is negligible. Therefore, we can exploit the correlation between  $y[n]$  and  $x[n]$  to adapt  $\beta$ . The proposed adaptation algorithm can be expressed as

$$\beta[n+1] = \beta[n] - \lambda[n] \times \{y[n]x[n]\}, \quad |\beta| < 1 \quad (15)$$

where  $\lambda[n]$  is a time-varying step-size. To speed up the convergence rate, we choose the time-varying step-size as [22]

$$\lambda[n] = \frac{\mu}{\phi[n]} \quad (16)$$

with  $\phi[n] = \rho\phi[n-1] + (1-\rho)x^2[n]$

where  $\mu$  is the constant step-size for adjusting the convergence rate,  $\phi[n]$  is an instantaneous power estimation of  $x[n]$  and  $0 < \rho \leq 1$  is the forgetting factor.

### 3.2 CWI detection and estimation algorithm

It has been shown that the transfer function  $H_B(z)$  from  $u[n]$  to  $x[n]$  has the bandpass property, and the corresponding frequency response has a maximum magnitude at the notch frequency [21]. Therefore, this transfer function can be expressed as

$$H_B(z) \triangleq \frac{X(z)}{U(z)} = \frac{1 + \alpha}{2} \frac{(1 - \beta)z^{-1}}{1 - \beta(1 + \alpha)z^{-1} + \alpha z^{-2}} \quad (17)$$

We use the above property to estimate the jamming power  $\hat{P}_J[n]$  as follows

$$\hat{P}_J[n] = \frac{\phi[n]}{G|H_B(e^{j\omega_n})|^2} \quad (18)$$

where  $G$  is the gain from the received antenna to the input of the ANF, and  $\phi[n]$  is defined in (16).

Moreover, we exploit the second-moment statistic value of  $\beta$  to detect whether the CWI appears. From (15) and (18), we have

$$\text{var}(\beta) \triangleq \sigma_\beta^2 \simeq \frac{\mu^2 \sigma_w^2}{\phi} \simeq \frac{\mu^2 \sigma_w^2}{\hat{P}_J G |H_B(e^{j\omega_n})|^2} \quad (19)$$

where  $\text{var}(\cdot)$  denotes the variance operator, and  $\sigma_w^2$  denotes the power of AWNG  $\tilde{w}(t)$ . When CWI is detected,  $\sigma_\beta^2$  becomes very small. Ideally,  $\beta$  converges to a fix value:  $\cos(\omega_n)$ . Thus,  $\sigma_\beta^2$  can be calculated by the sample mean and sample variance of  $\beta$  with the  $N_\beta$ -point of  $\beta$  and can be expressed as follows

$$\hat{\sigma}_\beta^2 = \frac{1}{1 - N_\beta} \sum_{n=1}^{N_\beta} (\beta[n] - \bar{\beta})^2 \quad (20)$$

with  $\bar{\beta} = \frac{1}{N_\beta} \sum_{n=1}^{N_\beta} \beta[n]$

$N_\beta$  is essentially a sensitivity parameter. A larger  $N_\beta$  leads to more accurate estimation of  $\beta$  but causes longer detection delay. This parameter should be carefully chosen, especially for the cases of detecting a rapidly changing pulsed CWI.

```

1: procedure CWI D&E( $N_\beta, \nu, \beta[n], N_F, f_s$ )
2:    $n \leftarrow 1$ 
3:    $\beta[n] \leftarrow \beta_{init}$ 
4:    $\Delta f \leftarrow f_s/N_F$ 
5:    $\mathbf{J} \leftarrow \{\Phi\}$ 
6:   for  $n = 1 \rightarrow N_\beta$  do
7:      $\beta[n+1] \leftarrow \beta[n] - \lambda[n]y[n]x[n]$ 
8:   end for
9:    $\bar{\beta} \leftarrow \frac{1}{N_\beta} \sum_{n=1}^{N_\beta} \beta[n]$ 
10:   $\hat{\sigma}_\beta^2 \leftarrow \frac{1}{1-N_\beta} \sum_{n=1}^{N_\beta} (\beta[n] - \bar{\beta})^2$ 
11:  if  $\hat{\sigma}_\beta^2 \leq \nu$  then
12:     $\hat{f}_J = \frac{f_s}{2\pi} \cos^{-1}(\bar{\beta}[n])$ 
13:     $\hat{B} = \lceil \hat{f}_J / \Delta f \rceil$ 
14:     $\mathbf{J} \leftarrow \{\mathbf{J}, \hat{B} \pm 1, \hat{B}\}$ 
15:     $\tilde{R}_i[l] \leftarrow |R_i[l]|$ 
16:    return DECT = 1,  $\mathbf{J}$ , and  $\tilde{R}_i[l]$ 
17:  else
18:    return DECT = 0
19:  end if
20: end procedure

```

Fig. 3 CWI detection and estimation algorithm

```

1: procedure CWI NULLING( $\mathbf{J}, \tilde{R}_i[l]$ )
2:   for  $k \in \{\mathbf{J}\}$  do
3:     if  $|R_i[k]| \leq |\tilde{R}_i[k]| \times \delta$  then
4:        $\mathbf{J} \leftarrow \{\mathbf{J} \setminus k\}$ 
5:     else
6:        $R_i[k] \leftarrow 0$ 
7:     end if
8:   end for
9: end procedure

```

Fig. 4 CWI nulling algorithm



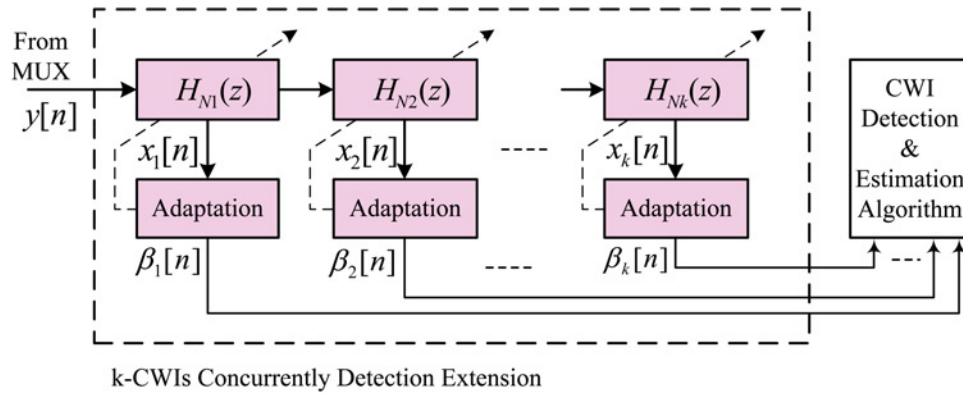


**Fig. 5** Extension version of the proposed hybrid approach

**Table 1** Performance metrics against  $N_F$

Algorithm	$N_F = 256$			$N_F = 512$			$N_F = 1024$		
	$\Gamma$ , dB	$P_d$ , %	$\tilde{\Gamma}$ , dB	$\Gamma$ , dB	$P_d$ , %	$\tilde{\Gamma}$ , dB	$\Gamma$ , dB	$P_d$ , %	$\tilde{\Gamma}$ , dB
N-sigma [10]	5.54	0.90	<b>0.05</b>	5.61	8.95	<b>0.50</b>	6.63	82.52	<b>5.47</b>
CME [11]	5.72	40.11	<b>2.29</b>	6.06	80.20	<b>4.86</b>	6.72	98.00	<b>6.59</b>
proposed	6.83	84.19	<b>5.75</b>	7.84	95.64	<b>7.50</b>	8.8	97.56	<b>8.59</b>

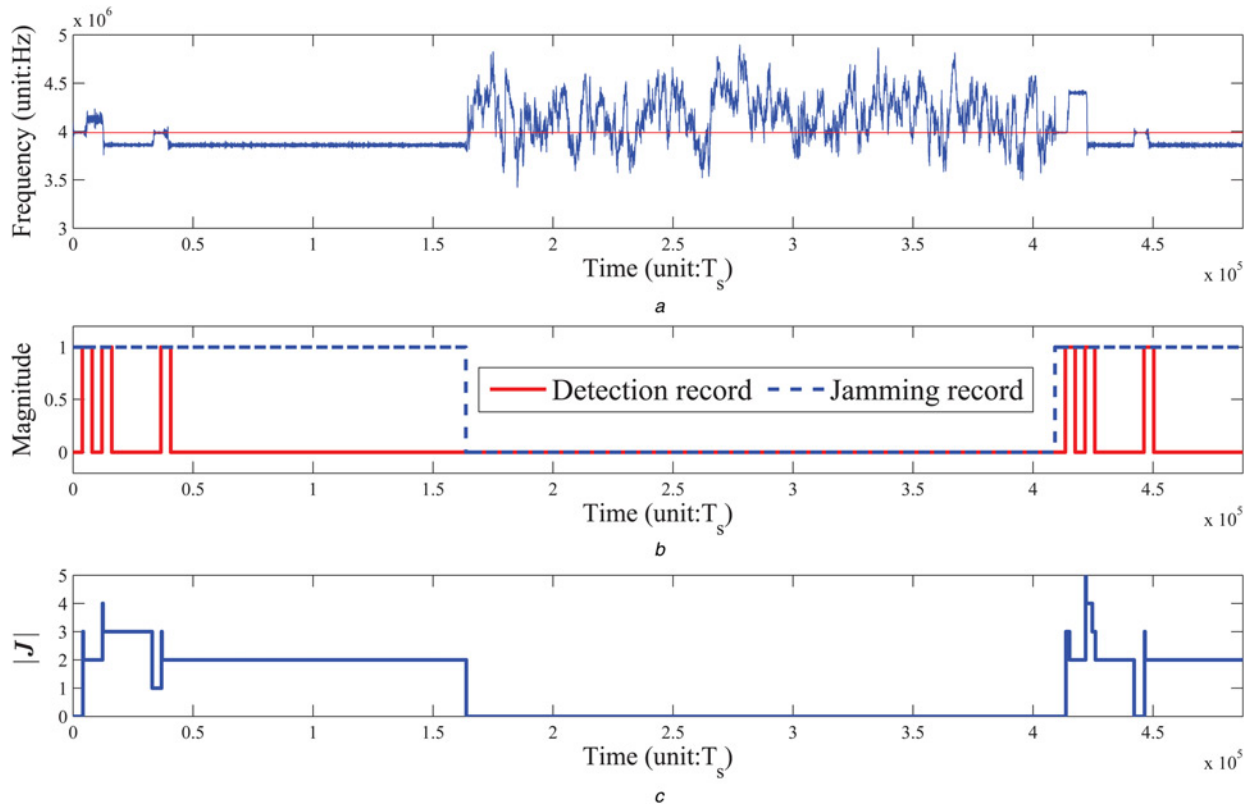


**Fig. 6** Example of a single pulsed CWI detection and estimation processes  
a CWI estimation process  
b CWI detection process  
c Number of bins in the null pool

In addition, we need to predefine a threshold parameter  $\nu$  and then periodically calculate  $\text{var}(\beta)$ . If  $\nu > \text{var}(\beta)$ , we claim that no CWI is detected. The detection probability of the proposed CWI detection algorithm is defined as

$$P_{\text{det}}(\nu) = P(\hat{\sigma}_\beta^2 \leq \nu | \text{CWIs present}) \quad (21)$$

In the case that CWIs are detected, we can estimate the jamming frequency as follows

**Table 2** Parameters of the four Jammers and the resulting null pool

$i$	$\text{JSR}_i$	$f_{J,i}$ , MHz	$B$	Estimated polluted bins
1	25	4.192	65.6	{65, 66}
2	35	4.092	64.0	{64}
3	30	3.992	62.4	{62, 63}
4	40	4.310	67.4	{67, 68, 69, 70}

$$\hat{f}_J = \frac{f_s}{2\pi} \cos^{-1}(\bar{\beta}) \quad (22)$$

where  $f_s$  is the sampling frequency and  $\bar{\beta}$  is obtained using (20). Therefore the estimation of the polluted frequency bin is

$$\hat{B} = \lfloor \hat{f}_J[n] / \Delta f \rfloor \quad (23)$$

where  $\Delta f = f_s / N_F$  denotes the frequency resolution. To summarise, Fig. 3 shows the pseudo-code of the proposed CWI detection and estimation algorithm.

### 3.3 CWI nulling algorithm

Since the proposed hybrid SIC scheme is a feedback approach, we need to check whether the jamming CWI still presents before nulling the polluted frequency bins in the nulling pool  $J$ . Therefore, we check magnitude variation in all frequency bin

indices  $k$  in  $J$  by the following equation

$$|R_i[k]| \leq |\tilde{R}_i[k]| \times \delta \quad (24)$$

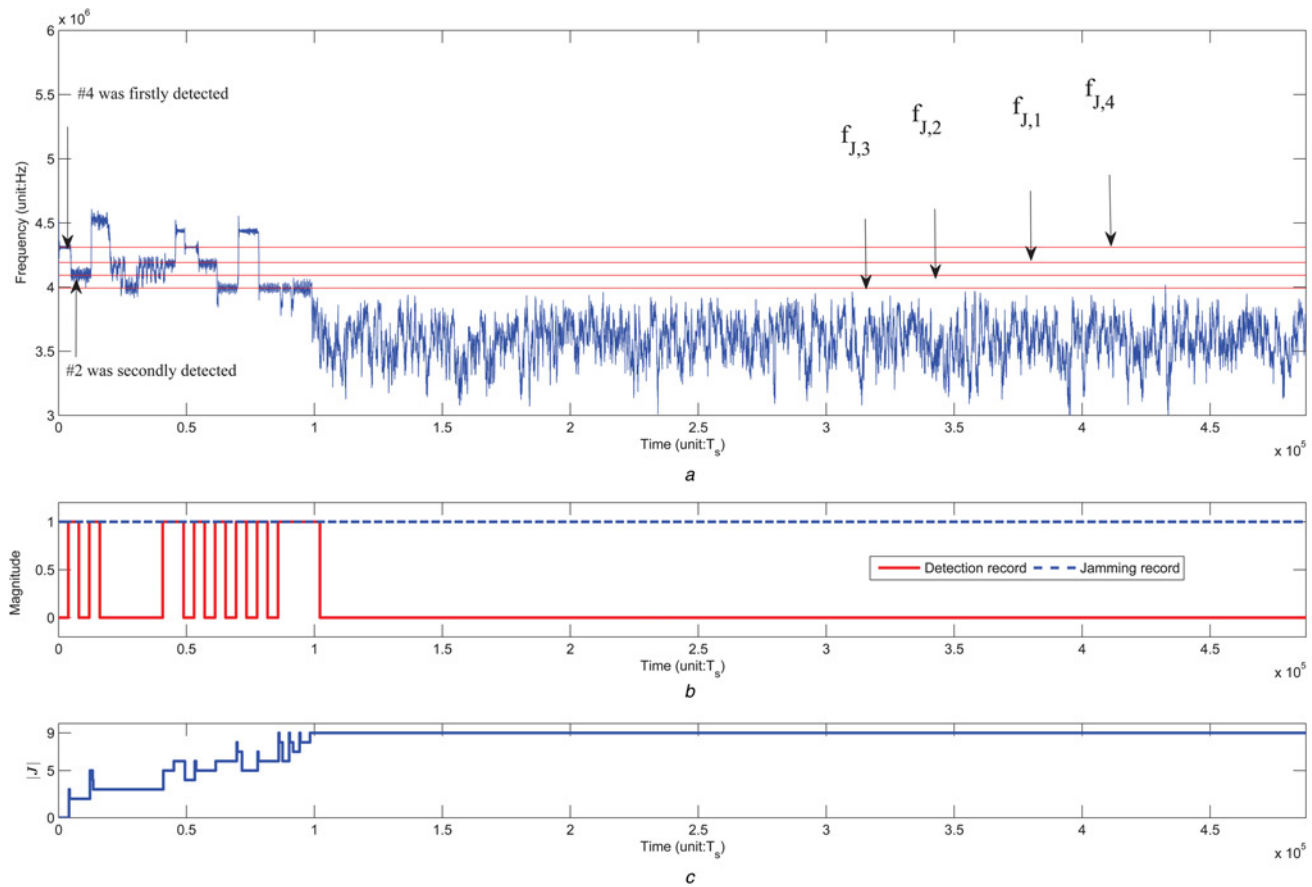
where  $0 < \delta \leq 1$  is a system parameter and  $|\tilde{R}_i[k]|$  is the recorded magnitude of the detected CWI. If the current magnitude of the estimated polluted frequency bins  $|R_i[k]|$  is much less than it was in the previous iteration, we may assume that the CWI has disappeared. In this case, we remove this index from  $J$ . After checking all bins in  $J$ , we then null all remaining bins by setting  $R_i[k] = 0$ . To summarise, Fig. 4 expresses the pseudo code of the proposed CWI nulling algorithm.

### 3.4 Concurrent multiple CWIs detection

To detect more than one CWI in one iteration, we can simply modify the TDIDE block as shown in Fig. 5. By cascading the  $k$ -stage IIR filters, the multistage configuration will notch the  $i$ th strongest CWI at the  $i$ th IIR filter during the adaptation processing. If the number of CWIs is greater than or equal to the number of stages, the estimated jamming frequency at each stage can be expressed as

$$\hat{f}_{J,i} = \frac{f_s}{2\pi} \cos^{-1} \left( \frac{1}{N_\beta} \sum_{n=1}^{N_\beta} \beta_i[n] \right) \quad (25)$$

The corresponding frequency bins are  $\hat{B}_i = \lfloor \hat{f}_{J,i} / \Delta f \rfloor$  for  $i = 1, \dots, k$ .

**Fig. 7** Example of CWIs detection and estimation processes

a CWI estimation process

b CWI detection process

c Number of bins in the null pool

#### 4 Simulation results

In this section, we show the performance of the proposed hybrid successive CWI cancellation scheme and compare the scheme with the conventional  $N$ -sigma-based algorithm [10] and CME algorithm [11]. The performance metrics we used have been defined in Section 2.4. First, we compare the anti-jamming capability with 256-, 512- and 1024-point FFTs. Next, we focus on the anti-jamming capability with a 256-point FFT, in which we can validate that our approach can achieve better performance than the conventional algorithms.

The parameters used in the simulation are described below. For the analogue front end, the bandpass filter in the analogue front end is a sixth-order Butterworth filter with a centre frequency of 4.092 MHz and a bandwidth of 2.046 MHz. The automatic gain controller is adjusted every 5 ms. A 5-bit ADC with a sampling rate of 16.368 MHz is used. We consider that the values of  $C/N_0$  are between 35 and 55 dB-Hz.

For the CWI detection IIR filter, the parameters used by the adaptation for  $\beta$  are:  $\mu = 2^{-6}$  and  $\rho = 1 - 2^{-6}$ ; the  $-3$  dB bandwidth parameter  $\alpha = 0.9878$ ; the sensitivity parameter  $N_\beta$  used in (20) is 4096; and the system parameter  $\delta$  used in (24) is 0.5. With the target JSR above 17 dB and  $C/N_0$  above 45 dB-Hz, we choose  $0.5 \times 10^{-3}$  as the threshold  $v$ , so that the detection probability is greater than 90% [17].

For the jamming source, the frequency of the CWIs is randomly chosen within the pass-band of the Butterworth filter, that is,  $f_{J,i} \in [3.069, 5.115]$  MHz, and the phase of the CWIs is randomly chosen from 0 to  $2\pi$  rad, that is,  $\theta_{J,i} \in [0, 2\pi]$ .

##### 4.1 Anti-jamming capability with various numbers of FFT points

We choose three different values of FFT points to evaluate the impact of the frequency resolution on the anti-jamming algorithms. In addition, the number of jamming sources is 8, and the JSR of each jamming source is randomly chosen between 20 and 35 dB. The acquisition results are obtained using 1 ms non-coherence integration with a data length of 10 ms. Table 1 shows the Monte Carlo simulation results over  $10^4$  iterations. The table shows that our hybrid-domain approach with  $N_F = 256$  has 5.7 and 3.46 dB improvements compared to the  $N$ -sigma algorithm [10] and CME algorithm [11], respectively. As expected, with a larger  $N_F$ , the frequency domain statistics become more accurate; hence, the performance improvements become smaller.

##### 4.2 Anti-jamming capability for pulsed CWI with a 256-point FFT

To verify our CWI detection and rejection ability for pulsed CWI, we assume only one pulsed CWI with a JSR of 35 dB presents, that is,

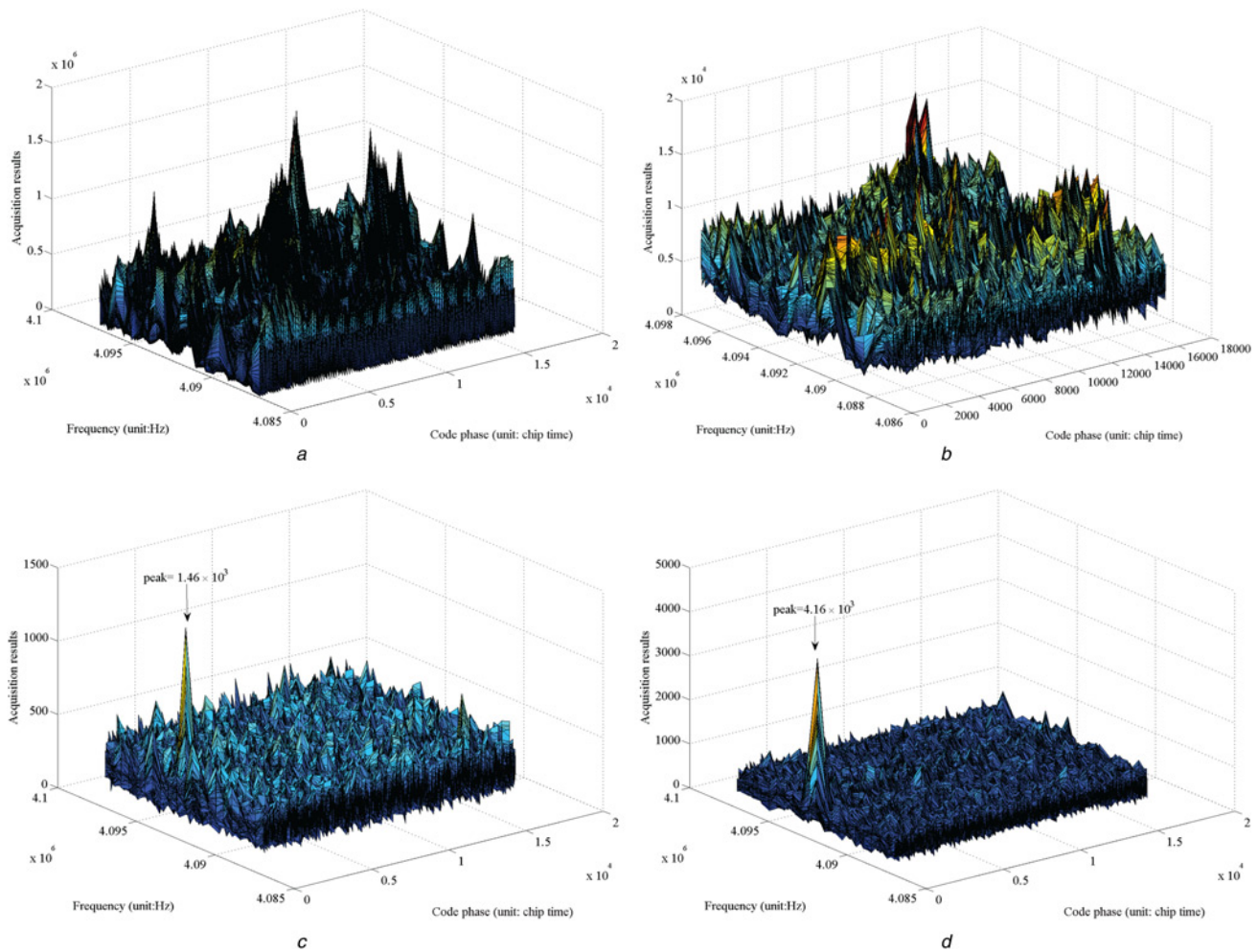


**Fig. 8** Comparison of acquisition results  
a No CWI rejection approach is applied  
b  $N$ -sigma algorithm [10]  
c CME algorithm [11]  
d Proposed hybrid scheme

$K = 1$ . The true jamming frequency  $f_J$  is 3.9886 MHz (the straight line in Fig. 6a), and the corresponding frequency bin is  $B = 62.4$ . However, owing to the finite frequency resolution, the jamming bins should be approximately 62–64. The behaviour of the pulsed CWI is shown in the dotted line in Fig. 6b. The pulsed CWI appears at the beginning of the simulation, disappears between the times of  $1.63 \times 10^5$  and  $4.09 \times 10^5$  units, and then reappears.

The resulting estimated jamming frequency is shown in Fig. 6a. Accompanied by the detection record shown in Figs. 6a and b shows that, when we detect the CWI, the estimated frequency is close to the true jamming frequency. However, a few type-II detection errors occur for the frequency of approximately 4.04 MHz, which corresponds to bins {68, 69, 70}. We can see that, at a time of  $4096 T_s$ , the jamming signal is detected, and the corresponding frequency bins are {62, 63, 64}; when the pulsed CWI disappears at a time of  $1.63 \times 10^5$ , our algorithm removes all frequency bins, that is,  $J = \{\emptyset\}$ , with a processing delay of  $4096 T_s$ ; when the pulsed CWI returns at a time of  $4.09 \times 10^5$  units, our algorithm again detects three frequency bins, that is, {62, 63, 64}; in addition, the false alarms result in a larger null pool so that  $J = \{63, 64, 68, 69, 70\}$ . However, these false alarms are dissolved at a time of  $4.24 \times 10^5$  units, and finally the frequency bins in the null pool are {63, 64}. The variation in the number of elements in the null pool  $J$  is shown in Fig. 6c.

#### 4.3 Anti-jamming capability comparison for multiple CWIs with a 256-point FFT

Table 2 shows the parameters of the four CWIs used in this simulation. Because of the finite frequency resolution, one CWI may pollute multiple frequency bins. For example, jammer 1 with  $f_{J,1} = 4.192$  MHz may pollute frequency bins 65 and 66. The last column in Table 2 shows the estimated polluted frequency bins.

The successive CWI nulling processes are shown in Fig. 7a. As expected, the CWI with the greatest power will be detected and nulled first. In addition, as shown in Fig. 7b, we also observe that, after approximately  $10^5 T_s$ , these four CWIs are successively nulled and no further CWI has been detected at the input of the DSP block. Moreover, two type-II detection errors occur for the frequency near 4.42 MHz.

In addition, Fig. 8 shows the acquisition results among different anti-jamming approaches. The results show that the  $N$ -sigma algorithm [10] fails with  $N_F = 256$ , and the CME algorithm [11] can acquire a peak value of  $1.46 \times 10^3$ ; however, the proposed hybrid scheme can achieve a peak value of  $4.16 \times 10^3$ . Fig. 8 also shows that the type-II detection errors do not affect the functionality of the acquisition process.

## 5 Conclusions

In this paper, we have presented a novel anti-jamming architecture for GPS receivers. The proposed anti-jamming method is a hybrid approach that successively detects and estimates CWIs in the time domain and nulls the detected CWIs in the frequency domain. We proposed using an adaptive second-order IIR filter as a detection and estimation module. The state variables used in the adaptation process are exploited to design our detection and estimation algorithm. Since the detection and estimation of CWIs are performed in the time domain, we can reduce the hardware complexity required in the frequency domain, for example, by reducing the number of FFT points. Simulation results have shown that the proposed hybrid approach has effective SINR improvements of 5.7 and 3.46 dB with respect to the  $N$ -sigma [10] and CME [11] algorithms when a 256-point FFT is used. The low required of FFT points benefits the proposed hybrid approach in the hardware implementation.

## 6 Acknowledgment

This work was supported in part by the National Science Council, ROC, under grant 101-2218-E-197-001.

## 7 References

- [1] Rhodes C.: 'Future spectrum demands will impact DTV and GPS receiver designs', *IEEE Trans. Consum. Electron.*, 2012, **58**, (1), pp. 8–14
- [2] Balaei A.T., Dempster A.G., Presti L.L.: 'Characterization of the effects of CW and pulse CW interference on the GPS signal quality', *IEEE Trans. Aerosp. Electron. Syst.*, 2009, **45**, (4), pp. 1418–1431
- [3] Kaplan E.D.: 'Understanding GPS: principles and applications' (Arctech House, 2006, 2nd edn.)
- [4] Liu Y., Ran Y., Ke T., Hu X.: 'Code tracking performance analysis of GNSS signal in the presence of CW interference', *Signal Process.*, 2011, **91**, (4), pp. 970–987
- [5] Evans-Pughe C.: 'Jam today', *Eng. Technol.*, 2011, **6**, (4), pp. 78–81
- [6] Wang Z.-S., Lv M., Tang B.: 'Paper application of partial coefficient update LMS algorithm to suppress narrowband interference in DSSS system'. Proc. Int. Conf. Electronic Measurement & Instruments, February 2009, pp. 275–278
- [7] Balaei A.T., Dempster A.G.: 'A statistical inference technique for GPS interference detection', *IEEE Trans. Aerosp. Electron. Syst.*, 2009, **45**, (5), pp. 1499–1509
- [8] Zhang L., Yuan S., Chen Y., Yang J.: 'Narrowband interference suppression in DSSS system based on frequency shift wavelet packet transform'. Proc. Int. Conf. Communication Software and Networks, October 2009, pp. 333–337
- [9] Capozza P.T., Holland B.J., Hopkinson T.M., Landrau R.L.: 'A single-chip narrow-band frequency-domain excisor for a Global Positioning System (GPS) receiver', *IEEE J. Solid-State Circuits*, 2000, **35**, (3), pp. 401–411
- [10] Jining F., Siliang W., Ju W.: 'Narrow-band interference excision in spread-spectrum systems using new N-sigma algorithm based on fuzzy threshold', *J. Syst. Eng. Electron.*, 2009, **20**, (1), pp. 20–26
- [11] Henttu P., Aromaa S.: 'Consecutive mean excision algorithm'. Proc. IEEE Int. Symp. Spread Spectrum Techniques and Applications, September 2002, pp. 450–454
- [12] Saarnisaari H.: 'Consecutive mean excision algorithms in narrow-band or short time interference mitigation'. Proc. Int. Symp. Position Location and Navigation, April 2004, pp. 447–454
- [13] Rusch L.A., Poor H.V.: 'Narrowband interference suppression in CDMA spread spectrum communications', *IEEE Trans. Commun.*, 1994, **42**, (2/3/4), pp. 1969–1979
- [14] Gunturi S., Balakrishnan J.: 'Mitigation of narrowband interference in differentially modulated communication systems'. Proc. IEEE Int. Acoustics, Speech and Signal Processing, April 2009, pp. 2549–2552
- [15] Ma W.-J., Mao W.-L., Chang F.-R.: 'Design of adaptive all-pass based notch filter for narrowband anti-jamming GPS system'. Proc. IEEE Int. Symp. Intelligent Signal Processing and Communication Systems, December 2005, pp. 305–308
- [16] Borio D., Camoriano L., Presti L.L.: 'Two-pole and multi-pole notch filters: a computationally effective solution for GNSS interference detection and mitigation', *IEEE Syst. J.*, 2008, **2**, (1), pp. 38–47
- [17] Chien Y.-R., Huang Y.-C., Yang D.-N., Tsao H.-W.: 'A novel continuous wave interference detectable adaptive notch filter for GPS receivers'. Proc. IEEE Int. Conf. Global Telecommunications Conf., December 2010, pp. 1–6
- [18] Villanti M., Pedone R., Corazza G., Crescimbeni R.: 'Joint time–frequency domain interference mitigation for Galileo L1 band receivers'. Proc. IEEE Int. Symp. Spread Spectrum Techniques and Applications, August 2006, pp. 238–242
- [19] Borio D., Camoriano L., Savasta S., Presti L.L.: 'Time–frequency excision for GNSS applications', *IEEE Syst. J.*, 2008, **2**, (1), pp. 27–37
- [20] Harris F.: 'On the use of windows for harmonic analysis with the discrete Fourier transform', *Proc. IEEE*, 1978, **66**, pp. 51–83
- [21] Regalia P.A.: 'Adaptive IIR filtering in signal processing and control' (Marcel Dekker, 1995)
- [22] Mvuma A., Nishimura S., Hinamoto T.: 'Adaptive IIR notch filter with controlled bandwidth for narrow-band interference suppression in DS-CDMA system'. Proc. IEEE Int. Symp. Circuits and Systems, May 2003, pp. 361–364